Available online at www.sciencedirect.com
ScienceDirect
Journal of Power Sources 161 (2006) 753–760
JOURNAL OF POWER SOURCES
www.elsevier.com/locate/jpowsour

Intrinsic borohydride fuel cell/battery hybrid power sources

Jian Hong, Bin Fang, Chunsheng Wang *, Kenneth Currie

Center for Manufacturing Research, Department of Chemical Engineering, Tennessee Technological University, Cookeville, TN 38505, United States

Received 17 March 2006; received in revised form 4 May 2006; accepted 5 May 2006
Available online 21 June 2006

Abstract

The electrochemical oxidation behaviors of $NaBH_4$ on Zn, Zn–MH, and MH (metal-hydride) electrodes were investigated, and an intrinsic direct borohydride fuel cell (DBFC)/battery hybrid power source using MH (or Zn–MH) as the anode and MnO_2 as the cathode was tested. Borohydride cannot be effectively oxidized on Zn electrodes at the Zn oxidation potential because of the poor electrocatalytic ability of Zn for borohydride oxidation and the high overpotential, even though borohydride has the same oxidation potential of Zn in an alkaline solution. The borohydride can be electrochemically oxidized on Ni and MH electrodes through a 4e reaction at a high overpotential. Simply adding borohydride into an alkaline electrolyte of a Zn/air or MH/air battery can greatly increase the capacity, while an intrinsic DBFC/MH(or Zn)–MnO_2 battery can deliver a higher peak power than regular DBFCs.

Keywords: Direct borohydride fuel cells; Zn–air batteries; Ni–MH batteries

1. Introduction

Fuel cells (FCs), tomorrow's center pieces of clean energy systems, show promise as environmentally friendly electrochemical power sources for distributed cogeneration for building and transportation applications. Fuel cells are also considered a primary candidate power source for meeting the military requirements of 'digitization' of the battlefield and 'Silent Watch' operations because of their silent and high energy density characteristics. Among various fuel cell types, proton exchange membrane fuel cells (PEMFCs) exhibit good performance at low temperatures. However, PEMFCs require relatively pure hydrogen gas as the fuel and the present hydrogen storage and reformer technologies cannot meet the application requirement of H_2-PEMFC. Therefore, alternative hydrogen-carrying liquid fuels, such as methanol, have been considered for fueling PEMFCs directly. But the low cell voltage and power density due to poisoning of the anode during methanol oxidation and the phenomena of methanol crossover limit the application of direct methanol fuel cells (DMFCs).

Aqueous solutions containing sodium borohydride have been considered as a fuel for direct borohydride fuel cells (DBFCs) since 1960 because of their high energy density, high cell voltage and environmental friendliness. $NaBH_4$ oxidizes in an aqueous alkaline media, to BO_2^- and water, and generates eight electrons:

$$BH_4^- + 8OH \rightarrow BO_2^- + 6H_2O + 8e^- \quad (E^0 = -1.24\,V) \tag{1}$$

With the oxidation of $NaBH_4$ at the anode, the atmospheric oxygen is electrochemically reduced at the interface between the cathode catalysts and the aqueous electrolytes, and the electrons are consumed:

$$2O_2 + 4H_2O + 8e^- \rightarrow 8OH^- \quad (E^0 = 0.40\,V) \tag{2}$$

The overall cell reaction is as follows:

$$BH_4^- + 2O_2 \rightarrow BO_2^- + 2H_2O \quad (E^0 = 1.64\,V) \tag{3}$$

The theoretical cell voltage is about 0.4 V higher than that of the PEMFC, and the specific capacity and energy of $NaBH_4$ can reach to 5.67 Ah g^{-1} and 9296 Wh kg^{-1}, respectively.

The present technology still poses three main obstacles preventing the broad application of the direct borohydride fuel cells (DBFCs). First, is BH_4^- crossover from the anode to the cathode, resulting in deactivation of the cathode electrocatalyst, although BH_4^- crossover can be minimized by using a cation

* Corresponding author.
E-mail address: cswang@tntech.edu (C. Wang).

0378-7753/$ – see front matter © 2006 Elsevier B.V. All rights reserved.
doi:10.1016/j.jpowsour.2006.05.018

exchange membrane. Second, is the poor anodic efficiency of BH_4^- due to the chemical hydrolysis of BH_4^- (reaction (4)):

$$BH_4^- + 2H_2O \rightarrow BO_2^- + 4H_2 \quad (4)$$

Finally, as with other types of fuel cells, the response to instantaneous power load requirements of DBFCs is insufficient, even though the continuous power output is satisfactory. Therefore, DBFCs must be coupled to a high power battery, leading to the increased complexity of added: weight, volume, and cost.

Recently, it has been reported that a MnO_2 cathode catalyst can avoid the performance degradation of the cathode arising from BH_4^- crossover. This is due to the fact that the MnO_2 cathode not only exhibits high electrolytic activity for oxygen reduction in BH_4^- solutions, but it also does not demonstrate catalytic activities for electrooxidation and chemical hydrolysis of BH_4^- ions [2]. Unfortunately, none of the existing anode catalysts can satisfy both requirements of high catalytic activity to oxidation of borohydride and low activity to its hydrolysis reaction. Pt, Pd, Raney Ni, and metal-hydrides are good catalysts for both oxidation and hydrolysis of borohydride. Cu and Au are poor electrocatalysts for hydrolysis of borohydride, but their electrocatalytic activity for oxidation of borohydride are also low [3]. Being able to depress the borohydride hydrolysis (Eq. (4)) and accelerate the borohydride oxidation (Eq. (1)) is a key technology to improving the columbic efficiency of DBFCs. The effective way to restrain hydrogen evolution is either to directly use a material with a high hydrogen evolution overpotential as an electrode or to coat the high hydrogen overpotential material on the electrode surface. It was reported that Si added into $LmNi_{4.7}Mn_{0.22}$ hydride as a catalyst for DBFCs can depress the H_2 evolution, and results in an increase in utilization of the borohydride from 21.37% for the parent alloy to 95.27% [4]. Zn metal or Zn-based alloys (Zn–In, Zn–Ni, Zn–Bi) may also be a good choice for DBFCs because Zn is a very effective element in suppressing hydrogen evolution in an alkaline solution. Zn has also been successfully used as an anode for Zn/Ni, Zn/MnO_2, and Zn/air batteries. In addition, to use Zn directly as an anode in DBFCs, mixing Zn into metal-hydride electrodes may increase the utilization of the borohydride. If Zn also has a reasonable catalytic ability for the oxidation of borohydride, Zn DBFCs may have a high open-circuit potential and high efficiency. Interestingly, Zn can be electrochemically oxidized in the alkaline solution at exactly the same potential of the borohydride oxidation (Eqs. (1) and (5)), providing a theoretical capacity of 820 mAh g^{-1}. The Zn oxidation in the anode:

$$2Zn + 4OH^- \Leftrightarrow 2ZnO + 2H_2O + 4e^- \quad (E^0 = -1.24\,V) \quad (5)$$

Overall Zn/air cell reaction is as follows:

$$2Zn + O_2 \rightarrow 2ZnO \quad (E^0 = 1.64\,V) \quad (6)$$

The heavy loaded Zn catalyst at the anode and MnO_2 at the cathode can function as a rechargeable Zn/air battery (1085 Wh kg^{-1}) when the borohydride fuel is shut off, and as a rechargeable Zn/MnO_2 battery (428 Wh kg^{-1}) when both borohydride and oxygen (or air) are blocked. If the catalytic ability of Zn for the oxidation of borohydride is not strong enough, MH/MnO_2 DBFCs are another choice because MH/air(MnO_2) and MH/MnO_2 also function as batteries when the borohydride fuel is shut off or both borohydride and oxygen (or air) are blocked. Zinc and MH in the borohydride fuel cell may not only increase the continuous energy output by suppressing the hydrogen evolution, but it also serves as an intrinsic battery component to deliver additional energy. In addition, Zn, MH, and MnO_2 catalysts are much cheaper than Pt, which would greatly decrease the cost. The borohydride intrinsic fuel cell/battery in this robust power source will supply a baseload energy output, while the inside secondary Zn (or MH)/air or Zn (or MH)–MnO_2 battery elements supplies additional energy during periods of high demand. The robust fuel cell will perform the same functions as those of a more complex fuel cell/battery and fuel cell/battery hybrid systems with the advantages of lower weight, volume, and cost.

In this paper, a novel robust direct borohydride fuel cell architecture incorporating Zn/air or MH/air battery elements is fabricated where the anode is Zn, Zn–Ni, Zn–metal-hydride, or MH, and the cathode is MnO_2. The Zn or MH here has three functions: (1) catalysts for electrochemical oxidation of borohydride; (2) suppressing the hydrogen evolution on Zn; (3) energy storage.

2. Experimental

2.1. Preparation of a liquid alkaline cell

For the purposes of this experiment, the air electrodes used for DBFCs consisted of a catalyst layer and a gas diffusion layer. The gas diffusion layer was a 0.5 mm thick membrane containing carbon black Vulcan XC-72 (70 wt.%) and PTFE (30 wt.%) as wet proofing agent and binder. The carbon black and polytetrafluoroethylene (PTFE) was first mixed and ground in excess isopropanol. Then the mixture was placed onto a Ni-mesh substrate, followed by roll-pressing it at 100 kg cm^{-2} and then sintering it at 300 °C for 30 min to form a hydrophobic gas diffusion layer. The catalyst layer was a MnO_2 catalyst (60 wt.%) loaded on activated carbon black XC-72 (20 wt.%) and PTFE binder (20 wt.%) which was prepared by mixing the MnO_2–carbon black–PTFE composite with isopropanol to form a paste and then rolling the paste into the formed gas diffusion layer to form a 0.12 mm thick film. The air electrode was heated at 100 °C for 2 h and then pressed at 100 kg cm^{-2}. The heavy-loading of MnO_2 materials in the air electrode not only gave a satisfactory steady-state power output, but also delivered additional power stored in the charged MnO_2 electrodes when pulsed power was required and when the cell voltage fell below a threshold level [5].

Zn and metal-hydride (MH) electrodes were made by mixing the 75 wt.% active material powder (Zn, MH) and 25 wt.% carbon supported PTFE (60 wt.% PTFE/C) and ground in excess isopropanol for 1 h. The slurry was coated onto a Ni foam and then rolled twice after being dried at 80 °C for 2 h. The active surface area of the electrode was roughly 4 cm^2, and the active material loading in the electrode was approximately

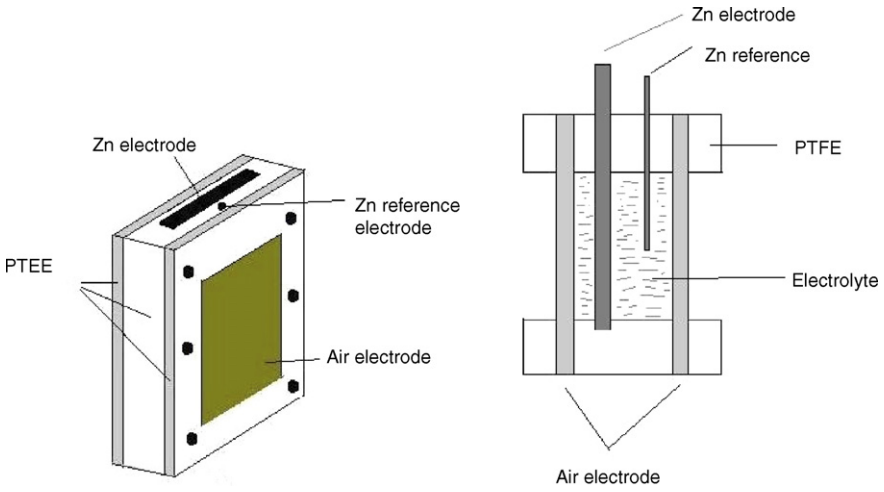

Fig. 1. Schematic illustration of the liquid alkaline cell.

15 mg cm^{-2}. To improve the catalytic ability of Zn for electrooxidation of borohydride, 10 or 50 wt.% of Zn in some cells was replaced by $LaNi_{4.7}Al_{0.3}$ and Ni powders.

Fig. 1 shows the schematic illustration of the liquid alkaline cell. The electrolyte is 7 M NaOH. A Zn wire was placed between the Zn anode and air cathode as a reference electrode to monitor the polarization of the anode. The fuel used for the direct borohydride fuel cell was 0.1 g $NaBH_4$ dissolved in 7 M NaOH solution to form 0.5 M $NaBH_4$–7 M NaOH solution.

2.2. Cell performance measurements

The discharge performances of the cells were measured using an Arbin Battery Testing System (College Station, TX) at room temperature. The electrochemical impedance spectroscopy (EIS) of the cell was measured from 100 kHz to 0.01 Hz at 5 mV potentiostatic signal amplitude using a Solartron 1287 electrochemical interface and a Solartron 1260 frequency response analyzer. The cell was normally discharged with the constant current of 4 mA cm^{-2} unless specified and the cut-off voltage was 0.7 V. The performance of the Zn–50 wt.% MH/MnO_2 (or MH/MnO_2) DBFC was obtained using linear polarization from open-circuit potential to 0.2 V (versus Hg/HgO) at a scan rate of 1 mV s^{-1} at 25 °C cell temperature. After each linear polarization scan, the electrodes (Zn–MH or MH) and 0.5 M $NaBH_4$–7 M NaOH electrolyte were replaced by fresh ones because some of the Zn and BH_4^- will be oxidized during linear polarization, resulting in a change in the composition of the electrode and electrolyte. Since the variation of the $NaBH_4$ concentration in NaOH is small during a linear polarization testing, the voltage–current of MH (or Zn–MH)/air cell in $NaBH_4$–NaOH electrolyte obtained using linear polarization can approximately be considered as a real DBFC performance. The peak power of the anodes in the Zn/air and MH/air cells in $NaBH_4$–NaOH electrolyte were measured under pulsed voltage conditions using the potential square-wave voltammetry program. In the potential square-wave voltammetry program, a Zn–50 wt.% MH and MH electrodes were stepped from an open-circuit potential to the different values, and then the corresponding current peak is measured. For convenience, all the anode potentials in the figures were converted to refer to Hg/HgO.

3. Results and discussion

3.1. Electrochemical reaction of borohydride on a Zn electrode

Since Zn and borohydride have the same oxidation potentials in the alkaline solution, the electrooxidation of borohydride on Zn was investigated by comparing the capacity of Zn electrode in the NaOH solution with and without borohydride addition. Fig. 2 shows the discharge behaviors of a Zn/air cell with and without 0.5 M borohydride addition in a 7 M NaOH electrolyte. The open-circuit voltages of the two cells were about 1.45 V, which is slightly lower than theoretical value (1.6 V) of oxidation of Zn and borohydride. At a discharge current of 4 mA cm^{-2}, a 1.2 voltage plateau was observed on both cells, which is a typical

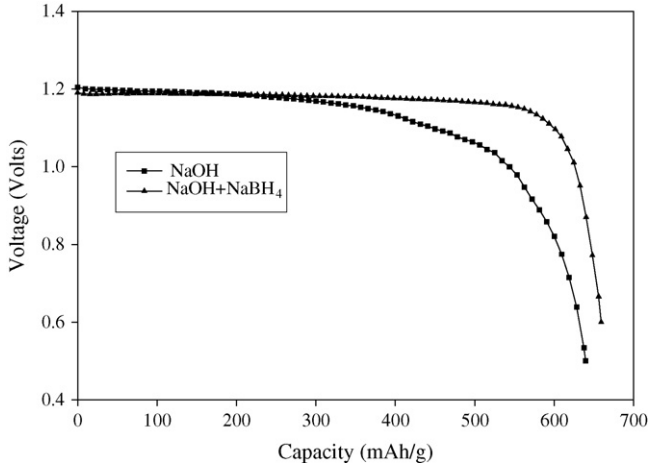

Fig. 2. The discharge behaviors of a Zn/air battery with and without 0.5 M borohydride addition in the 7 M NaOH electrolyte. Discharge current: 8 mA cm^{-2}.

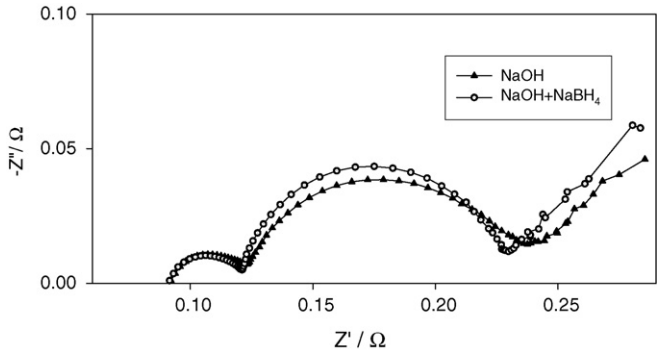

Fig. 3. Complex plane plots for the Zn electrode in a 7 M NaOH electrolyte with and without 0.5 M borohydride addition.

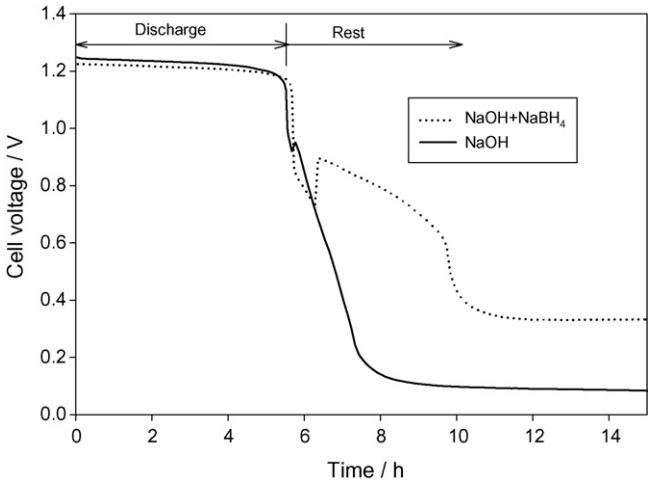

Fig. 4. Voltage profiles of Zn/air cells with and without 0.1 g $NaBH_4$ addition into 7 M NaOH electrolyte. Discharge current: 4 mA cm^{-2}.

behavior of the electrochemical oxidation of Zn in a Zn/air cell [6]. The discharge voltage plateau of DBFC due to oxidation of borohydride is about 1.0–0.8 V which depends on the discharge current and metal catalysts. The much lower voltage (1.0–0.8 V) when compared to the theoretical value (1.6 V) of Zn oxidation is attributed to polarization. If borohydride was also electrochemically oxidized at the 1.2 V voltage plateau, the capacity of the Zn/air cell with borohydride addition should be higher than the cell without borohydride. However, Fig. 2 indicates that the borohydride addition in the electrolyte only slightly increased the capacity of the Zn/air cell, which indicated that the electrochemical oxidation of borohydride on the Zn is very slow. It only extended the 1.2 V voltage plateau. The gradual decrease in voltage for a Zn/air cell at the end of discharge is attributed to the formation of a thin passivation film on the Zn electrode surface, which blocks the diffusion of the oxidation products species from the reaction sites, resulting in high diffusion polarization at the end of discharge [7]. To investigate the role of Zn in oxidation of borohydride, reaction kinetics of a Zn electrode in a three-electrode cell (Zn as the reference electrode) with and without borohydride addition was investigated using electrochemical impedance spectroscopy as shown in Fig. 3. The impedance in Fig. 3 was measured after discharging the cell to 200 mAh g^{-1}, and then resting for 1 h. The impedance of Zn shows two semicircles in the high frequency region, followed by the slope diffusion line. The high-frequency semicircle is attributed to the charge transfer reaction, while the middle-frequency semicircle is due to a passivated ZnO film on the Zn surface [7,8]. If the electrooxidation of borohydride occurred on the Zn electrode surface, the size of first semicircle of the Zn electrode in the electrolyte with the presence of borohydride should be less than that without borohydride. However, the sizes of the first-high-frequency semicircle in both impedance curves were the same, which confirmed that no electrochemical oxidation of borohydride occurred on the Zn electrode at 1.2 V. The slightly smaller size of the second semicircle in the impedance of the Zn electrode with borohydride addition compared to the electrode without borohydride addition suggested that the borohydride slows down the ZnO formation on the Zn electrode, which, in turn, decreased the overpotential during the discharge process. The impedance in Fig. 3 explains the long voltage plateau of the Zn/air cell with the presence of borohydride in the electrolyte found in Fig. 2. It is believed that the borohydride can be oxidized on the Ni at the voltage of 0.9–0.7 V [1,9–11]. However, there was no voltage plateau at 0.9–0.7 V in Fig. 2, which indicated that the electrooxidation rate of borohydride on the Ni foam is much less than that required by the discharge current due to the small surface area of Ni foam. To verify this assignment, the two cells with and without borohydride addition were discharged at a low current of 4 mA cm^{-2} and then were cut-off when their voltage reached 0.7 V. Fig. 4 shows the voltage profiles of the two cells during discharge and relaxation. For the borohydride cell, there is a small voltage plateau at a voltage range from 0.9 to 0.7 V during discharge at a low discharge current, and a long voltage plateau (0.9–0.7 V) during the relaxation period. However, there is no second (below 1.0 V) voltage plateau for the normal Zn/air cell during discharge or during the relaxation period. The 1.0–0.7 V open-circuit voltage of the borohydride cell is due to the oxidation and hydrolysis of borohydride on the Ni foam.

3.2. *Electrochemical reaction of borohydride on Zn–Ni and Zn–MH electrodes*

There is no detectable oxidation of borohydride on the Zn at 1.2 V, which may be due to the low electrocatalytic ability of Zn. Therefore, 10 wt.% of Ni or MH ($LaNi_{4.7}Al_{0.3}$) was mixed into the Zn electrodes. Figs. 5 and 6 show the discharge performances of Zn–10 wt.% Ni and Zn–10 wt.% MH in a 7 M NaOH–0.1 gM $NaBH_4$ electrolyte at different discharge currents, respectively. In addition to the 1.2 V voltage plateau due to Zn oxidation, a new voltage plateau appeared at around 0.9–0.7 V which was a typical oxidation voltage of borohydride on the Ni and MH (metal-hydride) electrodes in DBFCs [1,9–11]. Therefore, the specific capacities at a voltage of 1.2 V in Figs. 5 and 6 were calculated by the weight of Zn and the specific capacity at the voltage of 0.9–0.7 V by weight of added borohydride in the electrolyte. The specific capacities (about 600 mAh g^{-1}) of Zn–Ni and Zn–MH electrodes at 1.2 V in NaOH–$NaBH_4$ electrolyte were similar to the capacity of the Zn electrode in NaOH, so

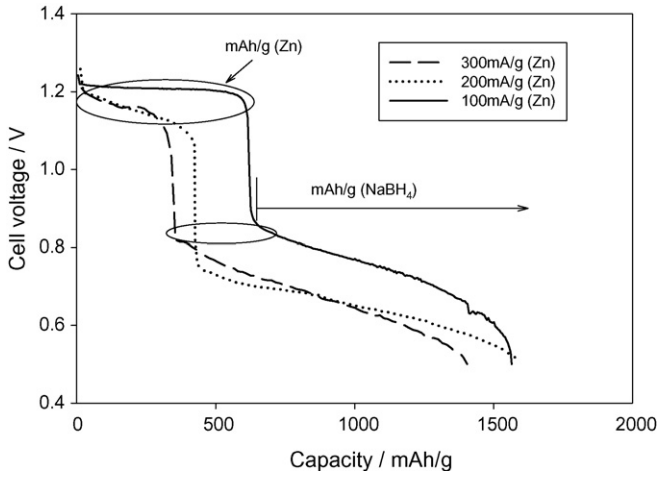

Fig. 5. Discharge curves of a Zn–10 wt.% Ni electrode in 0.1 g of $NaBH_4$–7 M NaOH solution at a current density of 4, 8 and 12 mA cm^{-2}. The loading of Zn in the electrode is 15 mg.

the catalytic ability of Ni and MH electrodes was still not strong enough to electrochemically oxidize the borohydride at 1.2 V. However, both catalysts can effectively catalyze the borohydride oxidation when the cell voltage was further decreased to 0.9 V as evidence of the second voltage plateau around 0.8 V in Figs. 5 and 6. Interestingly, the specific capacity of borohydride on the Zn–MH electrode (at the second voltage plateau) was larger than that on the Zn–Ni electrode. The total capacity of the Zn–10 wt.% MH electrode was slightly higher than Zn–10 wt.% Ni because $LaNi_{4.7}Al_{0.3}$ can absorb hydrogen and then electrochemically oxidize the absorbed hydrogen to form H_2O according to Eq. (7):

$$MH_x + xOH^- \leftrightarrow M + xH_2O + xe^- \quad (7)$$

In Figs. 5 and 6, the capacity due to the oxidation of $NaBH_4$ is much larger than the capacity of Zn oxidation. Therefore, adding a small amount of $NaBH_4$ into (Zn–Ni)/air and MH/air batteries can greatly enlarge their discharge capacities. Moreover, these

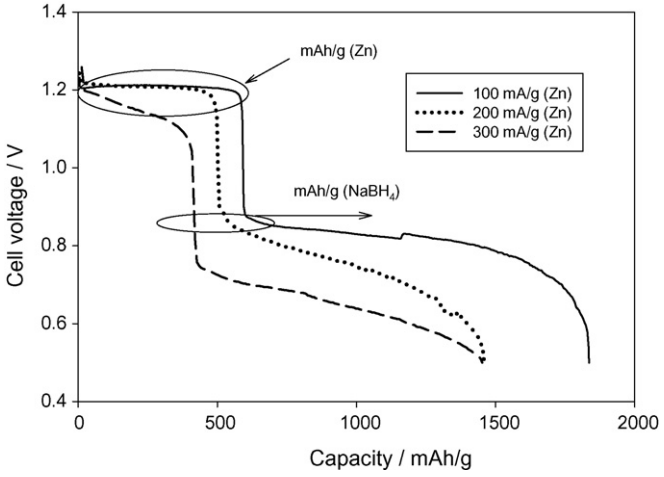

Fig. 6. Discharge curves of a Zn–10 wt.% $LaNi_{4.7}Al_{0.3}$ electrode in 0.1 g of $NaBH_4$–7 M NaOH solution at a current density of 4, 8 and 12 mA cm^{-2}. The loading of Zn in the electrode is 15 mg.

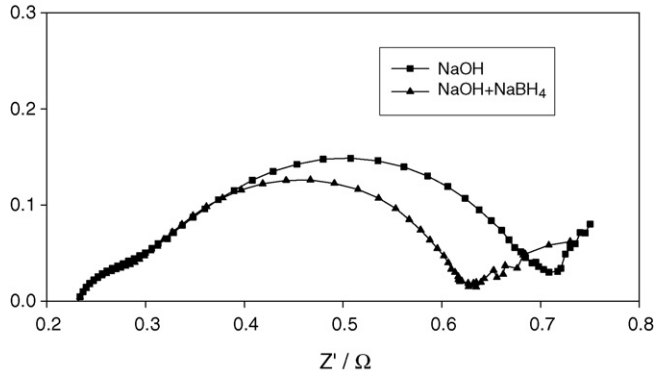

Fig. 7. Complex plane plots for Zn–10 wt.% MH electrodes measured at the middle of the first voltage plateau (discharge to 200 mAh g^{-1} in Fig. 6) in a 7 M NaOH electrolyte with and without 0.5 M $NaBH_4$ addition.

hybrid cells have a very high rate capability because the capacity of the cell is not sensitive to the discharge currents.

To understand the role of $LaNi_{4.7}Al_{0.3}$ and Ni in Zn–MH and Zn–Ni electrodes in the electrochemical reaction at the 1.2 and 0.8 V plateaus, EIS analyses were performed on the Zn–MH and Zn–Ni anodes at open-circuit conditions when the electrodes were discharged to the middle of the first and the second voltage plateaus with and without borohydride addition in the electrolyte. Fig. 7 illustrates the impedance spectra of the Zn–10 wt.% MH electrode measured after the electrodes were discharged to 200 mAh g^{-1} and rested for 1 h. The same sizes of the first semicircle for the Zn–MH electrodes in the electrolyte with and without $NaBH_4$ addition indicate that 10 wt.% $LaNi_{4.7}Al_{0.3}$ alloy in the Zn electrode did not improve the electrooxidation of $NaBH_4$ at 1.2 V, although it did decrease the impedance of the ZnO film on the Zn surface which is evident from the smaller size of the second semicircle for a Zn–10 wt.% MH electrode with 0.5 M $NaBH_4$ addition in the electrolyte compared to the same electrode in the electrolyte without $NaBH_4$ addition. Fig. 8 shows the impedances of the Zn–10 wt.% MH

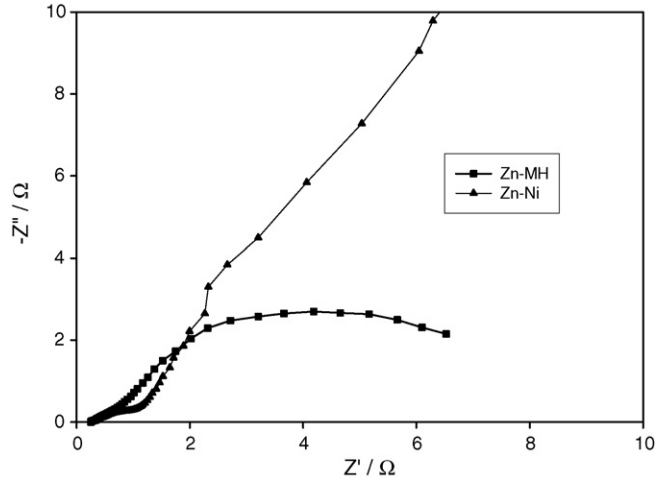

Fig. 8. The impedances of the Zn–10 wt.% MH and Zn–10 wt.% Ni electrodes in a 7 M NaOH–0.5 M $NaBH_4$ electrolyte. The impedances were measured after the electrodes were discharged to 2000 mAh g^{-1} (middle of the second voltage plateau) and rested at open-circuit for 1 h.

and Zn–10 wt.% Ni electrodes in a 7 M NaOH–0.5 M $NaBH_4$ electrolyte measured after the electrodes were discharged to 2000 mAh g^{-1} (at the middle of the second voltage plateau). Since the Zn has been oxidized in the first voltage plateau, Fig. 8 actually represents the electrooxidation impedance of $NaBH_4$ on the MH and Ni electrodes. The impedance of the Zn–Ni electrode in 7 M NaOH–0.5 M $NaBH_4$ electrolyte consisted of a high-frequency-depressed semicircle, followed by a sloped line in the low frequency range. The high frequency semicircle represents the charge-transfer reaction impedance and the low-frequency line is related to diffusion [12]. Different from the impedance electrooxidation of $NaBH_4$ on the Ni electrode, the reaction impedance on the MH electrode shows two depressed semicircles. The second depressed semicircle is properly attributed to the charge transfer related to oxidation of absorbed hydrogen into water (reaction (7)). The similar sizes of the first semicircle for Zn–Ni and Zn–MH suggest that both metals have a similar catalytic ability for the electrooxidation of $NaBH_4$ at 0.8 V.

It was suggested that the electrochemical oxidation reaction of $NaBH_4$ on the Ni and MH is a 4e reaction (reaction (6)), which will theoretically give 2821 mAh g^{-1} ($NaBH_4$) [1,3]. In Figs. 5 and 6, the utilization of $NaBH_4$ on the Zn–Ni and Zn–MH was only 50 wt.% of theoretical capacity, which may be attributed to the hydrogen evolution at the 1.2 V discharge plateau during Zn oxidation. To avoid the evolution of hydrogen due to the oxidation of Zn at 1.2 V and increase the utilization of $NaBH_4$, 0.05 g of $NaBH_4$ was added into the 7 M NaOH after the Zn–50 wt.% MH electrode was discharge to the second voltage plateau at 0.8 V (i.e. Zn was completely oxidized and MH began to discharge). The discharge profile of Zn–50 wt.% MH/air cell before and after $NaBH_4$ addition is shown in Fig. 9. The purpose of increasing MH content from 10 to 50 wt.% in the Zn–MH electrode was to improve the catalytic ability of the electrode for $NaBH_4$ oxidation. As expected, the utilization of $NaBH_4$ was increased to 98% when $NaBH_4$ was added at a low voltage. Also, the voltage of $NaBH_4$ oxidation (0.92 V) is higher than that of MH oxidation (0.8 V).

Although, the oxidation voltage of $NaBH_4$ is the same as that of Zn in alkaline electrolyte, the electrooxidation rate of $NaBH_4$ on Zn is much slower than that of Zn itself at the Zn oxidation voltage (1.2 V), which is probably due to the low catalytic ability of Zn for electrooxidation of $NaBH_4$. Adding MH or Ni into the Zn electrode did not enhance the catalytic ability for the electrooxidation rate of $NaBH_4$, but it accelerated the chemical hydrolysis rate of $NaBH_4$ at the Zn oxidation voltage, resulting in a low utilization of $NaBH_4$.

3.3. Battery and fuel cell performance of Zn–MH/air cell in $NaBH_4$–NaOH electrolyte

Since the catalytic activity of Zn for $NaBH_4$ oxidation is too low, Zn–MH and MH electrodes were selected to investigate the battery (energy storage) and fuel cell (energy conversion) performance. Zn–MH/air and MH/air cells with $NaBH_4$–NaOH electrolytes are the internal fuel cell/battery hybrid power source because Zn and MH electrode are energy storage materials (Zn/air and MH/air are batteries), MH is a catalyst for $NaBH_4$ oxidation and MnO_2 is the catalyst for oxygen reduction. The battery performance of the Zn–50 wt.% MH/air cell in the $NaBH_4$–NaOH electrolyte was measured by discharging the cell with constant current as shown in Fig. 10. $LaNi_{4.7}Al_{0.3}$ hydrogen storage material (MH) in Zn–50 wt.% MH can effectively catalyze the electrooxidation of $NaBH_4$ and absorb the hydrogen (charging) released from the hydrolysis of $NaBH_4$ [9], which is evident from the additional 4 h discharge time (125 mAh g^{-1} capacity) of $LaNi_{4.7}Al_{0.3}$ at 0.7 V, found in Fig. 10. A small amount (0.1 g) of $NaBH_4$ addition greatly increased the discharge time of the Zn–MH electrode. Normally, the alkaline electrolyte is an inactive material in the Zn/air (MnO_2) battery. It only serves as a conductor for OH^- and electronically separates the anode from the cathode. However, by simply dissolving borohydride into an alkaline electrolyte, the $NaBH_4$–NaOH electrolyte will also function as a fuel (active material) and greatly increase the cell energy as shown in Fig. 10. Similarly,

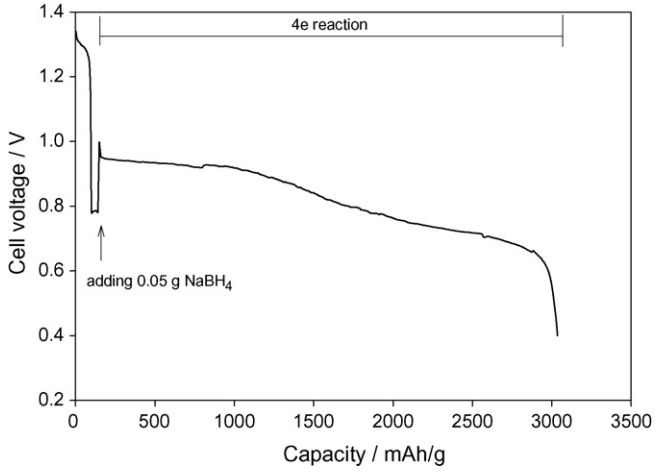

Fig. 9. Discharge profile of Zn–50 wt.% MH/air cell before and after 0.05 g $NaBH_4$ addition into 7 M NaOH. The specific capacity of the electrode is based on the weight of Zn–MH material before $NaBH_4$ addition and weight of $NaBH_4$ after $NaBH_4$ addition. Discharge current: 4 mA cm^{-2}.

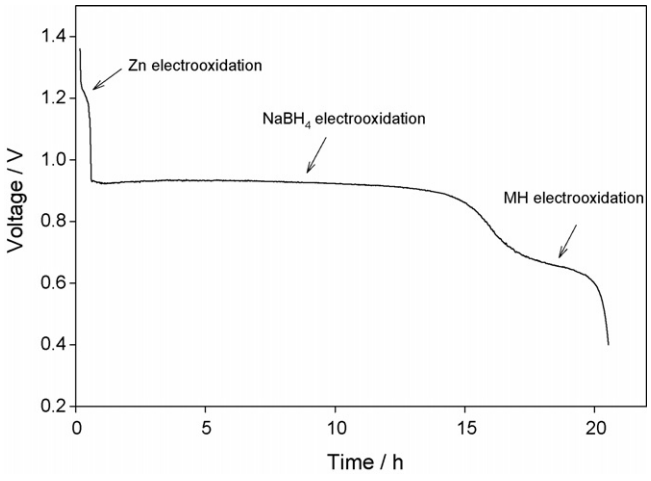

Fig. 10. The discharge performance of Zn–MH/air cell using 0.1 g $NaBH_4$–7 M NaOH as the electrolyte. The weight of Zn and MH ($LaNi_{4.7}Al_{0.3}$) are 0.3 g. The discharge current: 2.5 mA cm^{-2}.

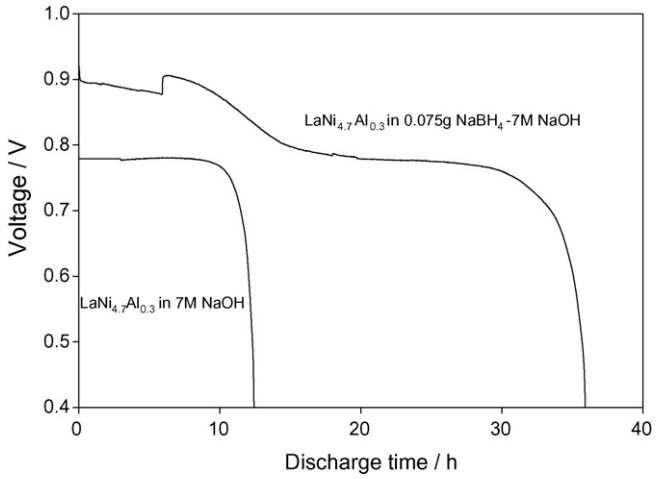

Fig. 11. The discharge performance of a MH/air cell in a 7 M NaOH electrolyte with and without 0.075 g $NaBH_4$ addition. The weight of the MH ($LaNi_{4.7}Al_{0.3}$) is 0.7 g. The discharge current: 2.5 mA cm^{-2}.

mixing borohydride into an alkaline electrolyte will also greatly enhance the energy of a MH–MnO_2 or MH/air cell (using MnO_2 as a cathode catalyst) as shown in Fig. 11. Figs. 10 and 11 also indicated that when the borohydride supplies are shut off, the cells will continue to supply power as a Zn/air or MH/air battery.

The fuel cell performance of Zn(MH)/air and MH/air cells using 0.5 M $NaBH_4$–7 M NaOH as a fuel and electrolyte was evaluated using linear polarization from open-circuit potential to 0.2 V at a scan rate of 1 mV s^{-1} at 25 °C (Fig. 12). The current density of the Zn–50 wt.% MH electrode is higher than that of the MH electrode due to the higher oxidation potential and capacity of Zn than that of MH. In our previous work [5], we demonstrated that H_2/O_2 alkaline fuel cells can be intrinsically hybridized with a MH/MnO_2 battery to form a high power internal hybrid power source by heavy loading of MH in the anode and MnO_2 in the cathode because both materials have a high energy storage capacity, and MH and MnO_2 are good catalysts for hydrogen oxidation and oxygen reduction, respectively. The result in Fig. 12 further shows that the H_2 fuel in the MH/MnO_2 fuel cell/battery hybrid power source can be replaced with borohydride fuel by simply dissolving borohydride into a circulating alkaline electrolyte, which will increase the energy density of the power source and simplify the system.

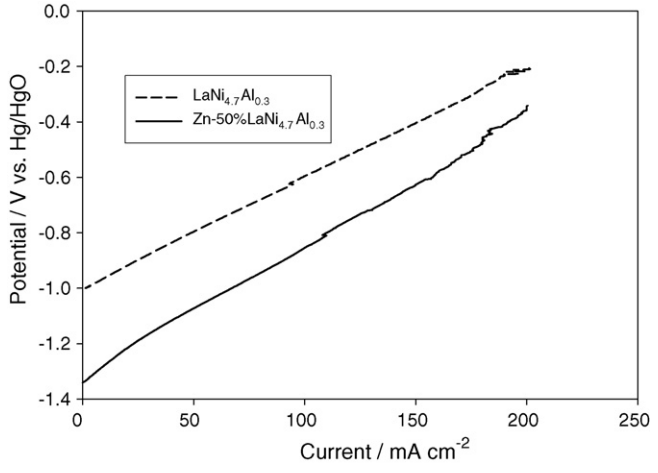

Fig. 12. The anode polarization of Zn(MH)/air and MH electrodes in a 0.15 M $NaBH_4$–7 M NaOH electrolyte measured using linear polarization at a scan rate of 1 mV s^{-1} at 25 °C. The Zn loading: 0.37 g, $LaNi_{4.7}Al_{0.3}$ loading in Zn–MH and MH electrode are 90 and 180 mg cm^{-2}, respectively.

The benefit of a fuel cell/battery hybrid power source is the high peak power to meet the instantaneous load requirement, which is often insufficient for fuel cells alone. When the cell voltage was suddenly stepped from the open-circuit potential (OCP) to a low voltage, an additional current should be supplied from the energy storage electrode. Fig. 13 graphs the current as a function of time of $LaNi_{4.7}Al_{0.3}$ electrodes in the alkaline electrolyte with and without $NaBH_4$ addition when the electrodes were stepped from OCP to different potentials. As expected, the peak currents of the electrodes in Fig. 13a are two times higher than the steady-state current, which is a typical performance of the energy storage electrode as shown in Fig. 13b. Similarly, the peak current of the Zn–50 wt.% MH electrode in a DBFC using a 0.5 M $NaBH_4$–7 M NaOH solution as a fuel and electrolyte

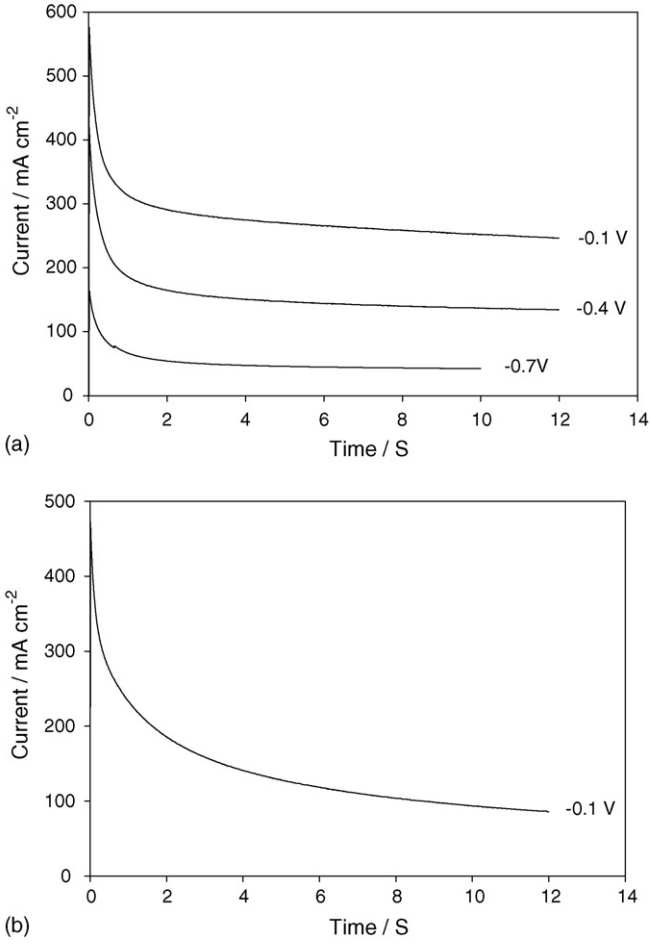

Fig. 13. The dependence of current density on time of a $LaNi_{4.7}Al_{0.3}$ electrode (a) with, and (b) without 0.2 M $NaBH_4$ addition into the 7 M NaOH electrolyte when MH electrodes were stepped from open-circuit potential to the different potentials. Anode MH loading: 375 mg cm^{-2}, MnO_2 loading in cathode: 180 mg cm^{-2}.

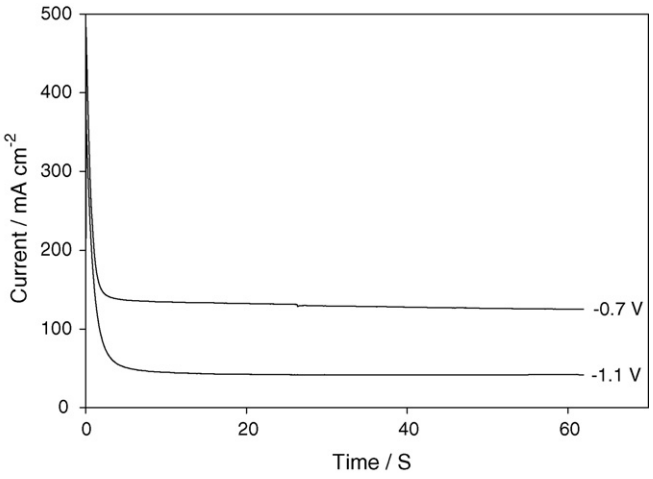

Fig. 14. The dependence of current density on time of a Zn–50 wt.% MH electrode in a 0.2 M $NaBH_4$–7 M NaOH electrolyte when the electrode was stepped from open-circuit potential to the different potentials. Anode Zn loading: 175 mg cm^{-2}, MH: 175 mg cm^{-2}, MnO_2 loading in cathode: 180 mg cm^{-2}.

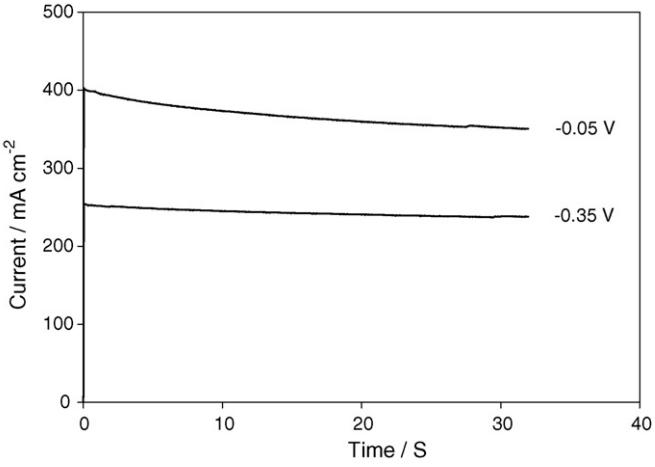

Fig. 15. The dependence of current density on time of a Ni electrode in a 0.2 M $NaBH_4$–7 M NaOH electrolyte when the Ni electrode was stepped from open-circuit potential to the different potentials. Anode Zn loading: 375 mg cm^{-2}, MnO_2 loading in cathode: 180 mg cm^{-2}.

was also measured when the electrode potential stepped from OCP (−1.34 V) to −1.1, and −0.7 V (Fig. 14). The peak current of the Zn–50 wt.% MH electrodes was even three times higher than the steady-state current. Therefore, the Zn/air battery in the Zn–MH/MnO_2 DBFC delivers additional peak current. Therefore, the DBFC using a Zn (or MH) anode and a MnO_2 cathode will form an intrinsic fuel cell/battery hybrid power source, giving a high peak power output as shown in Figs. 13 and 14. To confirm that the peak currents in Figs. 13 and 14 were induced from energy storage in the Zn and MH electrodes rather than the double layer in the porous electrodes, the current response of a Ni power electrode in 0.5 M $NaBH_4$–7 M NaOH solution was measured when Ni electrodes were stepped from an OCP to −0.05 and −0.35 V (Fig. 15). There is no peak current at the beginning of the potential steps, which indicates that the energy storage in the double layer capacitor due to the high surface area of a porous electrode is too low to give a peak current. All the peak current of a Zn and MH electrode in a DBFC is induced by the energy stored in the Zn and MH electrodes.

4. Conclusions

Although zinc can effectively compress hydrogen evolution and water hydrolysis, the low electrocatalytic ability for oxidation of borohydride on Zn also prevents the borohydride oxidation at the Zn oxidation potential. Adding borohydride into the alkaline electrolyte of a MH/air or Zn/air cell with MnO_2 as a cathode catalyst can greatly increase the energy of the batteries because of the electrochemical oxidation of borohydride. Similarly, a DBFC with heavy loading of the MH anode and MnO_2 cathode can function as an internal fuel cell/battery power source, which can deliver a high peak power.

References

[1] H. Dong, R. Feng, X. Ai, Y. Cao, H. Yang, C. Cha, J. Phys. Chem. B 109 (2005) 10896.
[2] R.X. Feng, H. Dong, Y.D. Wang, et al., Electrochem. Commun. 7 (2005) 449.
[3] B. Liu, Z. Li, S. Suda, Electrochem. Acta 49 (2004) 3097.
[4] L. Wang, C. Ma, X. Mao, J. Alloys Compd. 397 (2005) 313.
[5] C. Wang, A.J. Appleby, D.L. Cocke, Alkaline fuel cell with intrinsic energy storage, J. Electrochem. Soc. 151 (2004) A260.
[6] G. Zhang, X. Zhang, Electrochim. Acta 49 (2004) 873.
[7] M. Cai, S. park, J. Electrochem. Soc. 143 (1996) 3895.
[8] Y. Zheng, J. Wang, H. Chen, J. Zhang, C. Cao, Mater. Chem. Phys. 84 (2004) 99.
[9] S. Lee, J. Kim, H. Lee, P. Lee, J. Lee, J. Electrochm. Soc. 149 (2002) A603.
[10] J. Kim, H. Kim, Y. Jang, M. Song, S. Rajendran, S. Han, D. Jung, J. Lee, J. Electrochm. Soc. 151 (2004) A1039.
[11] B. Liu, Z. peng, S. Suda, Electrochim. Acta 49 (2004) 3097.
[12] E. Gyenge, Electrochim. Acta 49 (2004) 965.